Uncertainty Quantification of Modeled Electron Backstreaming Failure for the NEXT Ion Thruster

IEPC-2019-722

Presented at the 36th International Electric Propulsion Conference
University of Vienna • Vienna • Austria
September 15 – 20, 2019

John T. Yim[1], George J. Williams Jr.[2], Rohit Shastry[3], George C. Soulas[4]
NASA Glenn Research Center, Cleveland, OH, USA

Vernon H. Chaplin[5], and James E. Polk [6]
Jet Propulsion Laboratory, California Institute of Technology, Pasadena, CA, USA

Excessive electron backstreaming is one of the primary life-limiting failure modes for gridded ion thrusters. Physics-based modeling of the optics grid erosion and electron backstreaming margins is augmented with statistical uncertainty quantification techniques to generate a life expectancy distribution of this particular failure mechanism for the NEXT ion thruster. Generation of distributions instead of a single point estimate provide a more comprehensive picture of thruster failure probabilities and life expectation for various mission applications.

I. Introduction

HERITAGE aerospace hardware has typically approached life (or throughput, duration, cycles, etc.) qualification by one of two general philosophies, which will be labeled here as a safety margin approach and a probabilistic approach. The safety margin philosophy typically applies a relatively large factor-of-safety or margin (e.g. 1.5x throughput, 4x cycles, etc.) to the requirement value with the expectation that successful demonstration of this higher qualification value provides sufficient confidence in the flight hardware to readily achieve the lower requirement value. This approach implicitly assumes the failure distribution is far to the right of the requirement value which is buried in the small tail of the distribution—i.e. the width of the distribution is significantly smaller than the margin applied. The safety margin approach is attractive as it can be met with a single test or result (e.g. qualification test) and thus relatively simpler, faster, and cheaper to meet.

The underpinnings of the safety margin approach begin to fall apart when either the qualification life test becomes difficult or compromised (e.g. tests are too long and expensive and/or are affected by ground facility effects) or the requirement life cannot be assumed to lie in the far tail of the failure distribution. Both of these factors as well as a few others have been identified as issues in the traditional approach to life qualification for electric propulsion (EP) devices.[1] While wear or life testing is still necessary to identify and characterize failure modes, a probabilistic analysis approach is also recommended to better quantify the risk of failures and expected service life capability.[1] In particular, this approach should be applied for the primary wear-out failure mechanisms identified for EP technologies.

Past work has examined and updated the various failure mechanisms associated with NASA's evolutionary xenon thruster (NEXT) based on various tests and analyses.[2-4] Two failure mechanisms, pit-and-groove erosion and electron

[1] Aerospace technologist, Electric propulsion systems branch, john.t.yim@nasa.gov
[2] Research aerospace technologist, Electric propulsion systems branch, george.j.williams@nasa.gov
[3] Research aerospace technologist, Electric propulsion systems branch, rohit.shastry@nasa.gov
[4] Research aerospace technologist, Electric propulsion systems branch, george.c.soulas@nasa.gov
[5] Technologist, Electric propulsion group, vernon.h.chaplin@jpl.nasa.gov
[6] Principal engineer, Propulsion, thermal, and materials engineering section, james.e.polk@jpl.nasa.gov

backstreaming, were still in the process of having the analyses updated based on the data and results from the 51 kh long-duration test and other relatively recent assessments. These two failure modes are expected to be the primary wear-out mechanisms limiting the service life of NEXT. The results of the probabilistic life assessment of the electron backstreaming failure are reported here, while the pit-and-groove erosion analysis is ongoing and will be completed in the near future.

Accelerator grid aperture (or barrel) erosion leading to excessive electron backstreaming is one of the primary expected and experienced failure mechanisms for gridded ion thrusters.[5-7] Charge exchange (CEX) ions created in the near vicinity of the accelerator grid apertures can be accelerated toward the barrel walls and gradually sputter erode them. Eventually the apertures are widened enough where the resulting potential field will no longer sufficiently prevent electrons in the plume from streaming upstream into the discharge chamber. This leads to a loss in performance and ultimately in severe cases to overheating and failure of discharge chamber components, preventing the ability to sustain the discharge plasma. The electron backstreaming threshold is measured in practice where the total beam current increases typically by at least 1 mA while increasing the accelerator grid voltage towards the neutralizer common. The accelerator grid voltage at which this occurs is referred to as the electron backstreaming voltage (V_{ebs}). A soft failure criterion is defined here to be when V_{ebs} equals the nominal accelerator grid voltage set point. This is the start of measurable electron backstreaming, and the current increases dramatically with further changes in voltage past this threshold. As electron backstreaming is one of the primary expected failure mechanisms for gridded ion thrusters, an uncertainty quantification analysis was conducted to provide the probabilistic assessment of the service life capability as limited by this failure mode.

II. Analysis background and approach

Uncertainty quantification (UQ) explores the effects of the uncertainties of a model's input parameters on the resultant uncertainty of the outputs. In essence, it is an adaptation of evaluating uncertainty propagation for computational simulations or other analytical models. It should be clarified that there are multiple sources and types of uncertainties and errors involved, and how UQ does or does not explicitly handle each type. Perhaps the first distinction is to differentiate modeling assumptions and numerical errors from uncertainties in the physical input parameters. It is assumed that the underlying model has been sufficiently validated to assure that all of the pertinent physics are included in the model and the simplifying assumptions and approximations only have a second-order or higher effect on the results of interest. In addition, it is also assumed the model verification process also assures that the numerical parameters (e.g. grid discretization, time step, domain size, convergence criteria, etc.) are properly set to achieve a valid simulation result for each run.

For this UQ analysis, the underlying physics-based simulation of barrel erosion and electron backstreaming voltages are performed here with the CEX2D model code. CEX2D is a two-dimensional axisymmetric particle-based model of a single aperture and beamlet.[8] The model includes the capability to evolve eroded aperture geometries over time and to calculate the subsequent effects on electron backstreaming.[9,10] The model was further updated and then applied to the NSTAR thruster and exhibited successful comparisons to thruster aperture erosion and electron backstreaming data obtained during and after its life demonstration test (LDT) and extended life test (ELT) as shown in Figure 1.[11] It was then applied to the NEXT thruster and assessed against data from the NEXT 2kh wear test and the NEXT long-duration test (LDT) as shown in Figure 2.[11]

CEX2D incorporates, as all simulations, a number of physical approximations to provide a tractable solution to the problem at hand. These include, in part, 2D axisymmetry, the "flux tube" beam ion solution,[12] a disk emission neutral density model,[13] and simplified and semi-empirical approximations of sputter yields[14] and redeposition among others.[11] The relatively successful model correlation to the available wear test data shown in Figure 1 and Figure 2 across two different thrusters and four wear tests does show that these modeling approximations are not overly introducing issues with the ability to capture aperture erosion and electron backstreaming degradation. The differences seen here are generally lower than the range of the UQ results to be shown later, but of course additional margin can always be included in the results for critical mission applications to account for modeling and numerical errors. One item that will be revisited shortly below is that the approximations of the sputter yield and redeposition are tied to the uncertainty in the neutral number density that result in an overall effective erosion rate. The values of these parameters can be tied together in a consistent manner that provides repeatable acceptable correlation to the various wear test data. The model correlations across multiple thruster designs, operating points, test conditions, aperture locations, and wear durations provide confidence that the CEX2D model as applied for electron backstreaming calculations incorporates the appropriate physics and boundary conditions, reasonable modeling assumptions and approximations, and sufficient discretization and convergence parameters to proceed with the UQ analysis.

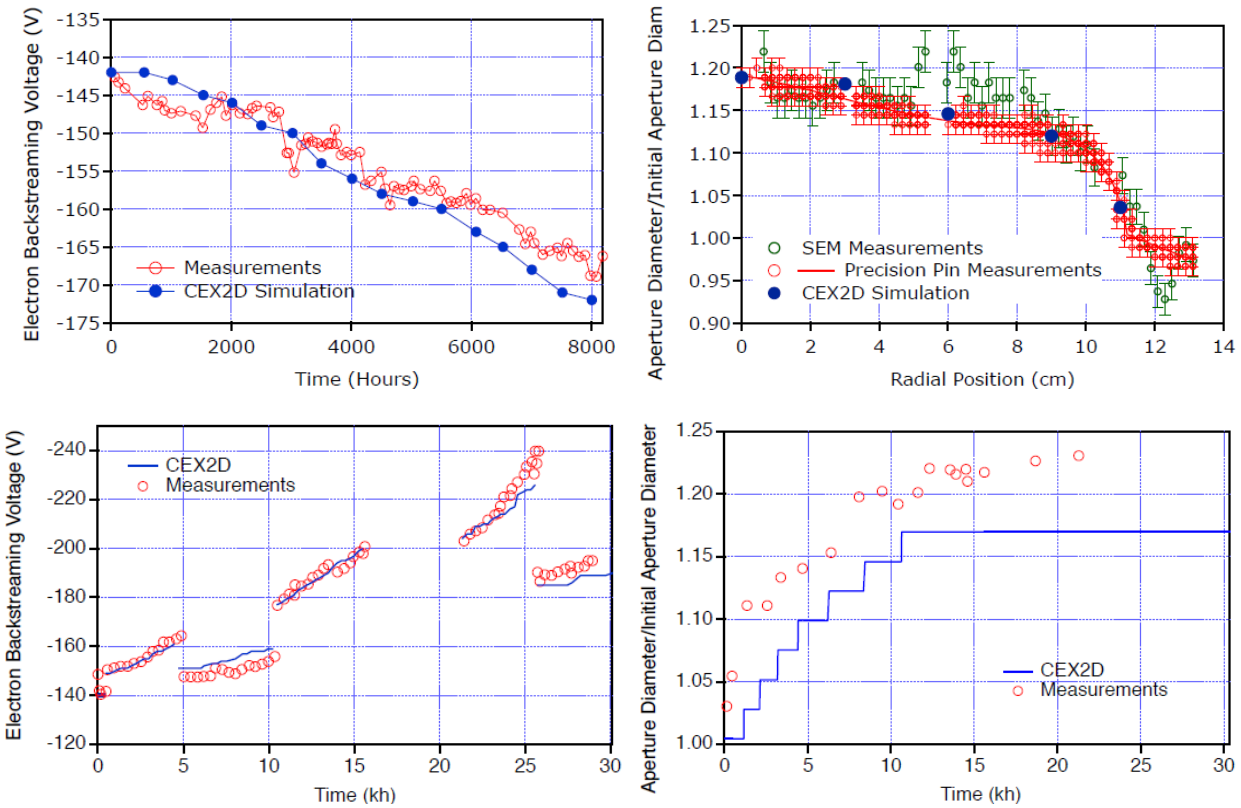


Figure 1: Comparisons between CEX2D results and measured V_{ebs} (left) and aperture diameters (right) for the NSTAR LDT (top) and NSTAR ELT (bottom)

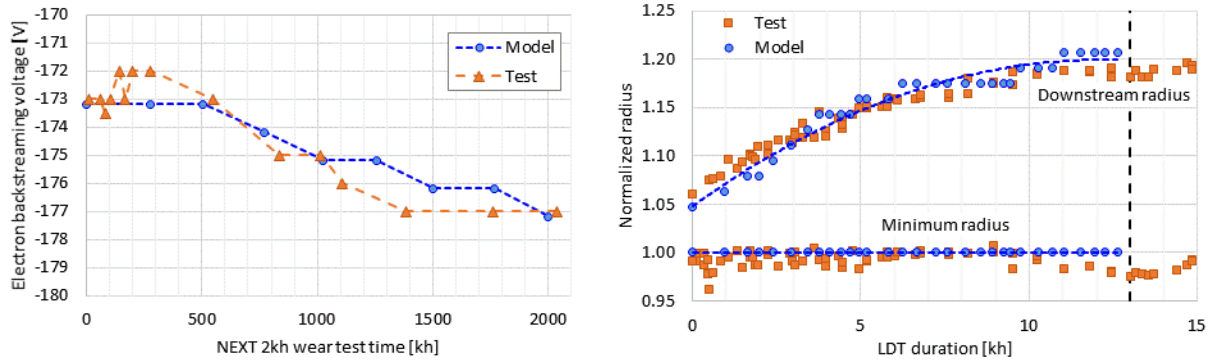


Figure 2: Comparisons between CEX2D results and V_{ebs} measured during the NEXT 2kh wear test (left) and aperture radii during the first segment of the NEXT LDT (right)

The UQ approach, then, examines the uncertainties involved with the physical-based input parameters including initial and boundary conditions. These uncertainties in the physical input parameters can be split into aleatory and epistemic uncertainties. Aleatory uncertainties are inherent variabilities always present for the situation at hand. For example, if multiple thrusters are assembled, variations in manufacturing runs will always result in at least slight differences in the geometries of the final hardware. Similarly, small differences in the discharge chamber and cathode from thruster to thruster will affect the discharge chamber plasma properties as will differences in the power processing unit (PPU) and propellant feed system. Tighter tolerances may help reduce some of these uncertainties to some extent, but at some level they will always be present. Epistemic uncertainties, on the other hand, are uncertainties due to a lack of knowledge. For example, if the electron temperature at the upstream or downstream boundary location has never been directly measured, there is some level of uncertainty with the values to assign for the model. Generally,

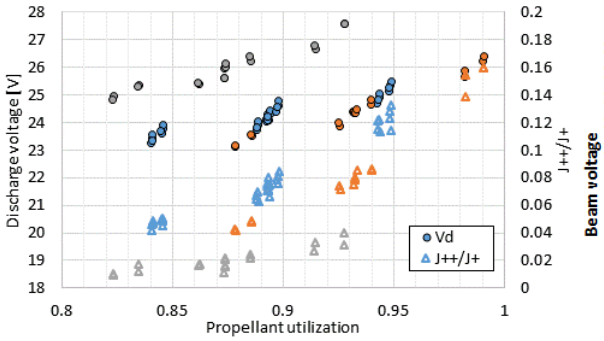
these parameters are estimated by extrapolation from available data, calculations from theory, or other engineering judgement. These uncertainties are reducible in the sense that a direct measurement would remove or reduce the uncertainty, but various reasons (e.g. lack of capability, funding, opportunity, etc.) may prevent such direct resolution. UQ is robust in the evaluation of the impact of aleatory uncertainties, but quantifying epistemic uncertainties is a more delicate task. It should be noted that all input parameters will have some level of both aleatory and epistemic uncertainties.

The CEX2D model has essentially fourteen physical input parameters and they are listed in Table 1 along with their respective sources of aleatory and epistemic uncertainties. The aleatory uncertainties are all modeled here to follow a normal distribution with the nominal value (mean) and variances based on specification values or measurement data where available. Where dispersion data are available from multiple thruster builds and tests in various published and unpublished data sets, the unbiased estimation of the standard deviation is used to prevent underestimation as sample sizes in some cases are relatively low ($n < 10$).[15] If very limited or no dispersion data are available, then the defined specification tolerances are used as an equivalent to a three standard deviation (3σ) level as a placeholder for now.

Table 1: CEX2D input parameters and uncertainties

Parameter		Basis of values	Aleatory uncertainties	Epistemic uncertainties
Grid gap (hot)	l_g	Optical measurements	Specification tolerance	Radial & TL extrapolation Measurement accuracy
Screen grid thickness	t_s	Drawing specification	Specification tolerance	Measurement accuracy
Screen grid aperture radius	r_s	Drawing specification	Dispersion data Specification tolerance	Measurement accuracy
Accel grid thickness	t_a	Drawing specification	Specification tolerance	Measurement accuracy
Accel grid aperture radius	r_a	Drawing specification	Dispersion data Specification tolerance	Measurement accuracy
Beam voltage	V_b	Throttle level setting	Specification tolerance	--
Accel grid potential	V_a	Throttle level setting	Specification tolerance	--
Discharge plasma potential	V_d	Internal measurements[16]	Dispersion data[21] Propellant utilization	Design level & TL extrapolation Measurement accuracy
Discharge electron temp.	Te_d	Internal measurements[16]	Dispersion data Propellant utilization	Design level & TL extrapolation Measurement accuracy
Beamlet current	j_b	Plume measurements[17,18]	Dispersion data	Plume to grid extrapolation Measurement accuracy
Double ion current fraction	j^{++}/j^{+}	Plume measurements[17,18]	Dispersion data Propellant utilization	Measurement accuracy
Discharge neutral density	n_n	Propellant utilization	Propellant utilization	Radial variation
Plume plasma potential	V_p	Plume measurements[19,20]	Dispersion data	Plume to grid & TL extrapolation Measurement accuracy
Plume electron temperature	Te_p	Plume measurements[19,20]	Dispersion data	Plume to grid & TL extrapolation Measurement accuracy

Each of the aleatory uncertainties are generally assumed to be independent of each other. However, there is a known and pronounced correlation of some parameters with the propellant utilization efficiency and ultimately the propellant mass flow rate.[22] The level of correlation used in the UQ analysis is based on sensitivity testing performed at the end of the NEXT LDT as well as other studies and tests performed with the NEXT thruster. The measured trends of these parameters are shown in Figure 3 for a few different operating conditions denoted by different colors. Here, an aleatory uncertainty is applied to the mass flow rate based on a notional specification tolerance of the mass flow controller accuracy, and then the dependent relations of the other parameters track this flow rate. Then extra sources of aleatory uncertainty—after the influence of propellant utilization is accounted for—are root sum squared (RSS) and used as an overall uncertainty value for these parameters.



Beam voltage	Beam current 1.00 A	1.20 A	1.60 A	2.00 A	2.35 A	2.70 A	3.10 A	3.52 A
1800 V		TL 12	TL 17	TL 22	TL 27	TL 32	TL 36	TL 40
1567 V		TL 11	TL 16	TL 21	TL 26	TL 31	TL 35	TL 39
1396 V		TL 10	TL 15	TL 20	TL 25	TL 30	TL 34	TL 38
1179 V		TL 09	TL 14	TL 19	TL 24	TL 29	TL 33	TL 37
1021 V		TL 08	TL 13	TL 18	TL 23	TL 28		
936 V		TL 07						
850 V		TL 06						
679 V		TL 05						
650 V		TL 04						
400 V		TL 03						
300 V		TL 02						
275 V	TL 01							

Figure 3: Trends of the discharge voltage and doubles-to-singles ratio with propellant utilization for a few select throttle levels (left) and the baseline TL settings for NEXT (right)

The epistemic uncertainties primarily arise from four types of extrapolation. There is uncertainty in radial variation of some of the parameters, where they are known either at only one location along the grid (e.g. center aperture) or in a global sense, but the profile radially along the grid is uncertain. There is uncertainty in the effect of throttle level (TL) on some of the parameters, where measurements at only a few select TLs may be available out of the nominal set of 40 TLs shown in Figure 3 for reference. There is uncertainty due to the maturity of the thruster design tested, where certain measurements were made only on earlier laboratory or engineering model hardware and not on flight-like versions. And there is uncertainty in extrapolating measurements made in the plume to the very near field region of the grids. In addition, there is of course always some finite uncertainty in the measurement accuracy, but these are generally relatively minor compared to the epistemic uncertainties from extrapolation assumptions.

It is important to discuss and assess these epistemic uncertainties to ensure the results of the following UQ analysis are not driven by these relative unknowns. For the grid thicknesses and aperture diameters, the measurement accuracy is minor relative to the aleatory uncertainty and can be assumed to be subsumed therein. Similarly, the measurement accuracy of the various plasma parameters are also relatively minor in comparison to the aleatory uncertainties and are effectively included there. The TL variations are handled by primarily examining the worst-case throttle levels as only a few TLs will drive the minimum service life limits. As will be shown later, this typically focuses on TL40 and TL37, which have the most test data available and remove this source of epistemic uncertainty in the evaluation of these worst-case scenarios. The thruster design level extrapolations apply only to the internal discharge plasma properties and an interval analysis using conservative estimates of minimum and maximum values show minimal impact of the discharge electron temperature and the discharge plasma potential. They are RSS'd into the aleatory uncertainties for conservatism, but results presented later below will again show minimal influence of these two parameters on the electron backstreaming service life. Similarly, the estimated epistemic uncertainty bounds in the downstream plasma potential and electron temperatures were evaluated by an interval analysis and did not exhibit strong influences on the results. The beamlet current is extrapolated from downstream plume measurements in an inverse sense where a beamlet plume model is used to iterate on beamlet current density profiles as a function of radius along the grid until the downstream profiles match measured data at various axial distances. This process minimizes the epistemic uncertainty in estimating the beamlet currents for a given location on the grid.

This leaves the radial variation epistemic uncertainties of the hot grid gap and the local neutral number density. For the hot grid gap, measurements at the center aperture location are available and since the center of the grid is the location of maximum erosion based on the current density profile peaking near the center, evaluation at the center provides a worst-case in terms of analyzing the service life capability. It should be noted that the initial limiting electron backstreaming location may not lie at the center, however. Using measurements of the cold grid gap profile along the grid radius, the relative hot grid gap along the radial profile is estimated and modeled. Successful matches to experimental values of the electron backstreaming voltage, shown above in Figure 2 and below in Figure 4, provide confidence the appropriate grid gap distances are implemented and the epistemic uncertainty reduced.

The final remaining, and perhaps largest, epistemic uncertainty is the neutral number density. While an overall average value can be calculated from propellant utilization, the radial profile along the thruster grid is unknown. The neutral number density has a direct correlation to the barrel erosion rate through the generation of charge exchange ions that impact the aperture barrel surfaces. It does not have any direct effect on the electron backstreaming voltage, however. It can then be combined with an assumed sputter yield relation, which has large epistemic uncertainties itself, into an effective single variable of the erosion rate. In other terms, if the erosion rate can be captured to a

sufficient accuracy, then the specific values of the neutral number density and sputter yields do not need to be resolved individually. This is only possible as these two variables primarily only affect the erosion rate, but no other factors in the CEX2D model—there are no other side effects of not knowing these two variables accurately apart from the erosion. Conceivably, a range of neutral number density and sputter yield combinations would be possible to achieve similar erosion rates. Here, it is found that using the nominal average neutral number density—calculated from mass conservation and propellant utilization efficiencies, applied across the radius of the grid based on the relative flatness of the beam profile—and the lower 50% likelihood sputter yield curve,[14] is sufficient to consistently capture the erosion rates across the two thruster designs and the different wear tests as shown above in Figure 1 and Figure 2.[11] This provides some level of confidence in the ability of the model to capture the loss of electron backstreaming margin over time and its implementation in this life assessment, but further resolution of these parameters and their uncertainties remains future work.

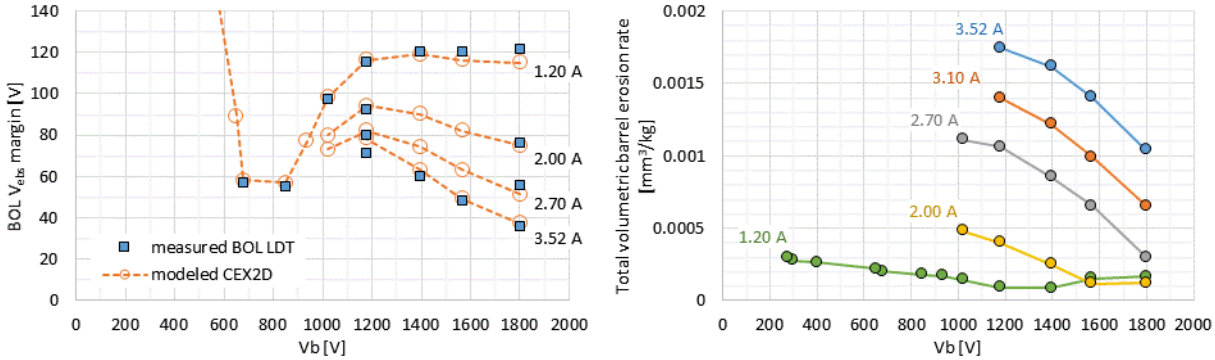


Figure 4: Nominal values of the beginning of life electron backstreaming voltage margins (left) and modeled BOL total volumetric barrel erosion rates (right) for the NEXT LDT configuration

For this service life analysis, which uses a model of a single aperture beamlet, the electron backstreaming threshold is set to be when the calculated electron backstreaming current for a single aperture exceeds 1% of that aperture's beamlet ion current. It is expected that electron backstreaming is a relatively local effect, occurring mostly at a few percent of the total number of apertures. For NEXT, a total backstreaming current of 1 mA requires approximately 3 – 12% (depending on the total beam current) of the apertures backstreaming 1% of their individual beamlet currents assuming the remaining beamlets have negligible backstreaming. It should be noted that around this inflection point in the accelerator grid voltage, the electron backstreaming current increases exponentially with voltage, so the nuances in determining V_{ebs} are expected to result in a discrepancy of 1 – 2 volts at most.

The service life throughput capability is affected by two separate factors: 1) the voltage margin between the accelerator grid voltage and the electron backstreaming voltage and 2) the overall erosion rate of the aperture walls gradually reducing the electron backstreaming voltage margin. In general, the same throttle point will not present a worst-case for both the V_{ebs} margin and barrel erosion rates. As shown in Figure 4 for the NEXT LDT thruster, TL40 presents the lowest beginning of life (BOL) V_{ebs} margin of around 35 V nominally with TL39 and TL36 following behind with nominal BOL starting margins below 50 V. For barrel erosion rates, also shown in Figure 4, the high beam current case is again generally worse, though this time the lower beam voltage conditions present the highest erosion scenarios with TL37 and TL38 having the fastest rates. The throughput capability is a function of both of these factors as shown in Figure 5 where some example simulation results highlight how the operational life is a function of both the erosion rate (the approximate slope of the line) and the initial V_{ebs} margin (the y-intercept at time zero). The cases shown in Figure 5 assume a single throttle level over the entire life. However, the worst-case scenario in terms of throughput limitation would be running in a high erosion mode (e.g. high slope at TL37) and then switching to a low V_{ebs} margin throttle point (e.g. TL40). This also means that electron backstreaming failure—presuming it does not immediately result in an irreversible overheating of a thruster component—is not a complete failure of the NEXT system, just an inability to operate at a particular TL with low V_{ebs} margin. Other TLs with higher voltage margins could still be operated for substantially longer durations in most cases.

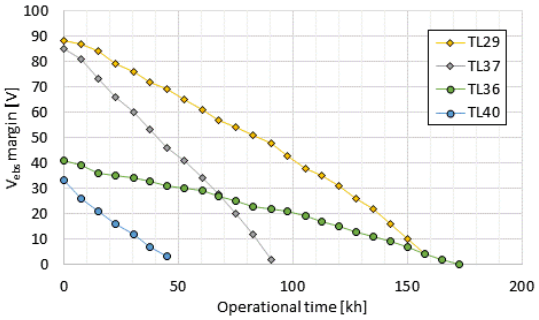


Figure 5: Example simulation runs showing reduction of the electron backstreaming margin as the aperture walls erode for different constant operation throttle levels

The CEX2D simulations assume the boundary conditions remain constant except for the grid thicknesses and aperture diameters. The grid positions, and thus the grid gap, are held constant in CEX2D. A decrease in grid gap was noted over the course of the NSTAR ELT and resulted in the relatively large changes in V_{ebs}.[23] However, the NEXT grids have implemented specific design features to minimize changes in the grid gap over time, as demonstrated in the NEXT LDT.[17,24] The constant grid gap in CEX2D, then, was determined to be acceptable for this NEXT service life assessment. Other changes in thruster conditions are expected to occur as the thruster wears. For example, as the accelerator grid apertures widen, the neutral losses will increase leading to impacts to the parameters influenced by propellant utilization as shown above in Figure 3, though the trends will be inverse since the propellant utilization is being affected by loss of neutrals instead of addition of neutrals from the propellant injection flow rate. Interestingly, however, neither significant nor consistent trends in discharge voltage changes were observed over the course of the different wear tests.[17,25-27] This is likely in part due to facility effects for at least the NEXT LDT, but also to the high sensitivity to propellant flow rates. As will be seen later, the parameters most affected by neutral losses have a relatively low impact on the electron backstreaming, at least within the expected range of changes. The one potential exception is the local neutral number density where the upstream discharge value will go lower, but the increased aperture size allows for greater throughput as well. The changes in the local neutral number density over time is assumed here to be in general subsumed by its epistemic uncertainty and that the prior correlations to wear tests over time show sufficient agreement for now. Future work should examine these areas in further detail.

For the following service life assessment of electron backstreaming, the reduction rate of the V_{ebs} margin is assumed to be relatively constant as approximated by the relatively linear nature of decrease as shown in Figure 5. To reduce the computational expense involved with running many simulations, the V_{ebs} reduction rate is assessed from shorter runs of approximately 25 kh in general. The error in extrapolating the rate from the initial 25 kh is on the order of 0.1 V/kh from the full length runs. No systemic offsets are observed, so this error will introduce some noise into the results and perhaps broaden the resultant distributions. Since the following analysis primarily focuses on the low life tail of the distributions, the results will be somewhat conservative. Further investigation of the impact of this extrapolation as well as effects of changes of the thruster over time are left for future work.

III. Results and discussion

The uncertainty quantification analysis was examined with both Latin hypercube sampling (LHS) and polynomial chaos expansion (PCE) techniques. LHS is a modified Monte-Carlo approach that is relatively robust to both dimensionality (number of variables) and the nature of the response of the output variables. By stratifying the random selection of input variable values to partitions of equal probability, it provides a more efficient means of performing a Monte-Carlo type analysis. PCE offers a potentially even more resourceful execution of UQ through establishing a surrogate model by taking advantage of polynominal series that are orthogonal to a weighting function with the same form as a given distribution function. For example, the Hermite polynomials are optimal for capturing the normal distribution form. This polynominal surrogate model, then, can be run using similar Monte-Carlo or LHS sampling techniques for many more orders of magnitude number of cases quickly compared to the original physics-based computational model. The PCE approach is somewhat limited in the number of dimensions (parameters) and type of output response it is effective for, so it is primarily beneficial for relatively targeted studies.

Both LHS and PCE approaches, particularly the latter, were primarily conducted using Sandia's Dakota analysis framework.[28] Due to the relatively large number of design parameters as listed above in Table 1, the LHS approach

was used first. Though not all fourteen parameters are expected to have significant influence on the throughput results, their aleatory variations are all included in the LHS runs for completeness. Later PCE runs focus only on the variables of higher significance, since PCE calculations are limited in the number of dimensions before they become more computationally expensive than LHS. The LHS evaluations are typically started with 100 simulation runs, though certain key TLs of note, for example TL40 and TL37, are run with several hundred more samples to help refine the statistics.

A set of LHS simulation runs for a single throttle level (TL40) over the life of the thruster is presented here first as an example of the UQ approach for generating the throughput capability distributions. The expected life capability for each case is calculated by the BOL V_{ebs} margin divided by the V_{ebs} reduction rate and multiplied by the mass flow rate for units of mass throughput. After ordering the results and applying an inverse beta distribution median rank, a discrete cumulative failure distribution is plotted as shown in Figure 6. The failure distribution is seen to be somewhat skewed with a long tail to the right. This arises from the nature of the throughput being inversely proportional to the barrel erosion rate or V_{ebs} reduction rate where low values will result in very long life. While Weibull distributions are commonly used to describe life and reliability data, other distributions that better capture skewed profiles including gamma and lognormal were also evaluated as was a ratio distribution of two normally distributed variables. For the gamma and Weibull forms, a maximum likelihood estimation approach via a Markov chain Monte Carlo calculation was used to evaluate appropriate shape and scale factors, while the mean and standard deviation were directly calculated from the data for the normal, lognormal, and ratio distributions evaluated here. A quantile-quantile (Q-Q) plot is also provided in Figure 6 showing that the gamma and lognormal distributions show in general the best comparisons to the results, particularly at the low end tail to the left which is the regime of higher interest here as it dictates the minimum expected life. These results have minor variations when performed for the data at different throttle levels, but in general the lognormal and gamma distributions provide the best fits around the minimum life tail. For consistency, the lognormal distribution will be used to approximate the expected throughput capability across the different TLs and scenarios examined via LHS. The benefit of having a fitted analytic distribution is that calculating the resultant summary statistics is then straightforward.

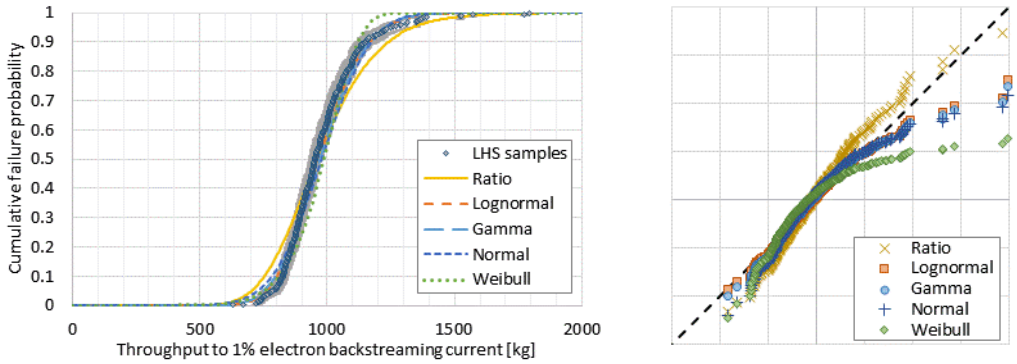


Figure 6: Median rank approximated and fitted analytical cumulative failure distributions (left) and Q-Q plot (right) for the LHS results versus fitted distributions for TL40 electron backstreaming throughput capability

The throughput capability is reported here as tolerance intervals for varying population proportions and confidence levels. One-sided tolerance intervals can be calculated from parameters of the fitted lognormal distributions.[29] The population proportion sets the expected percent of all NEXT thrusters to achieve a minimum throughput capability. The confidence levels result from estimating the fitted distribution from a finite number of simulation runs. Various confidence levels provide estimates of the range of what the true theoretical distribution would be for an infinite number of results. Table 2 lists a few select levels of both proportions for TL40 based on the results of the fit shown in Figure 6. More conservative (lower throughput) values will have high levels of both proportions. Based on a given mission and its guiding risk posture, an appropriate level of the tolerance interval can be applied to generate a corresponding throughput value to use in specific mission analyses. A similar approach was taken to assess TL37 as a single throttle level over the life of the thruster. Corresponding with the trends shown earlier in Figure 5, the higher starting V_{ebs} margin allows TL37 to process a substantially higher throughput before failure via electron backstreaming occurs despite its higher barrel erosion rate and faster rate of decrease of the V_{ebs} margin.

Table 2: Expected electron backstreaming throughput capability at a constant single throttle point (TL40 on left, TL37 on right) for various tolerance intervals

TL40	Confidence level		
Population	90%	95%	99%
50%	958 kg	956 kg	951 kg
90%	793 kg	790 kg	784 kg
95%	751 kg	748 kg	742 kg
99%	678 kg	674 kg	667 kg
99.7%	636 kg	632 kg	625 kg

TL37	Confidence level		
Population	90%	95%	99%
50%	1800 kg	1796 kg	1789 kg
90%	1536 kg	1531 kg	1521 kg
95%	1467 kg	1462 kg	1451 kg
99%	1346 kg	1340 kg	1328 kg
99.7%	1276 kg	1269 kg	1256 kg

As alluded to above, however, most missions will likely not run at just a single operating point and a feasible worst-case would be to run most of the mission at a high erosion throttle point and then require operation at a low V_{ebs} margin point. The UQ analysis is applied to these throttle level combinations through a simplified reduced order model approach where the distribution of the V_{ebs} margin reduction rate for a high erosion throttle level is paired with the distribution of BOL V_{ebs} margin for a low margin throttle point. The results of LHS runs across most of the throttle table, presented in Figure 7, provide the estimates of the worst TLs for either V_{ebs} reduction rate or the initial V_{ebs} margin. The general trends across the throttle table correspond to the trends shown earlier in Figure 4 for the nominal condition cases where the worst TLs for initial V_{ebs} margin trend to high beam current, high beam voltage points while the worst TLs for V_{ebs} reduction rate lie among the high beam current, lower beam voltage conditions. The analysis of the expected throughput for combination of TLs only holds if the trends of initial V_{ebs} margin and the V_{ebs} margin reduction rate do not present any correlation, but are rather independent of each other. For certain TLs, particularly the ones with a high beam voltage of 1800 V, some favorable correlation is seen where a lower initial V_{ebs} margin is more likely to also have a slower V_{ebs} reduction rate and vice versa where a faster reduction rate is more likely to have a higher initial margin. Other TLs with lower beam voltage do not exhibit any strong trends between the two outputs. Assessment of a relative independence or correlation between two different TLs was examined by running a set of LHS cases with the same variations in the input variables for TL40 and TL37, the worst-case TLs for initial V_{ebs} margin and the V_{ebs} margin reduction rate, respectively. Figure 7 shows no indication of a correlation between the two. Assuming relative independence between TLs for worst-case throughput assessment is supported by this worst-case combination result, and if anything is conservative for conditions where a favorable correlation exists as for the high beam voltage TLs. The resultant failure cumulative distribution functions (CDF) for a few worst-case scenarios of poor combinations of a high erosion TL with a low V_{ebs} margin TL are presented in Figure 8 with select tolerance interval values listed alongside in Table 3. Other scenarios not listed are expected to provide higher throughput capability than these worst-case limiting scenarios. It is recommended for missions that may approach these throughput levels to be assessed directly according to their specific throttle profiles to generate appropriate detailed service life estimates, distributions, probabilities, and margins.

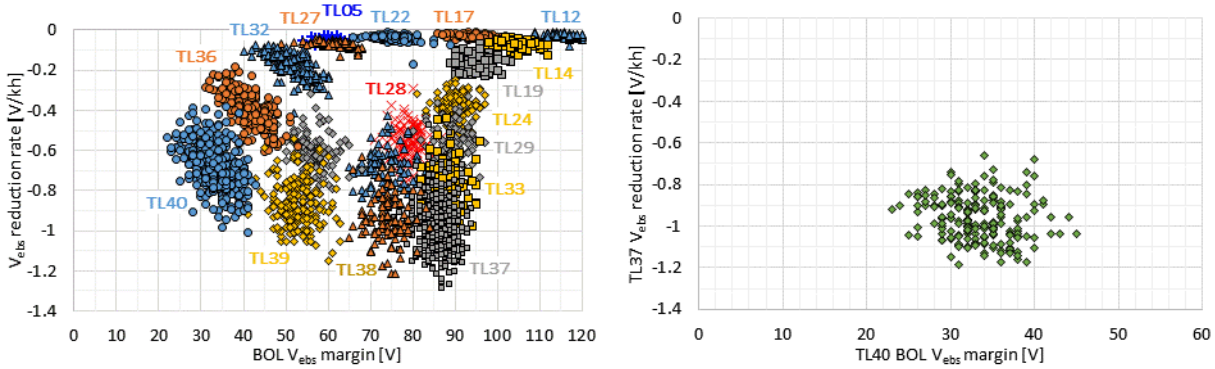


Figure 7: Throttle table trends based on LHS simulation results (left) and relative independence between TL40 and TL37 results for the same set of input parameter variations (right)

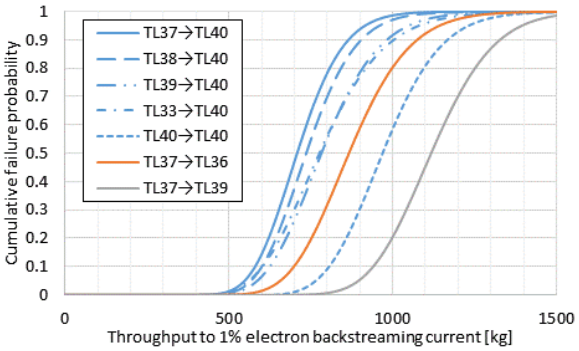


Figure 8: Throughput result CDFs for worst-case TL combinations

Table 3: Select tolerance intervals with a 95% confidence level for worst-case TL combinations

Erosion TL	Final TL	50% pop.	90% pop.	95% pop.
TL37	TL40	696 kg	565 kg	532 kg
TL38	TL40	715 kg	576 kg	540 kg
TL39	TL40	765 kg	605 kg	565 kg
TL40	TL40	956 kg	790 kg	748 kg
TL33	TL40	749 kg	571 kg	528 kg
TL37	TL36	850 kg	679 kg	636 kg
TL37	TL39	1100 kg	920 kg	873 kg

An alternative approach to fitting an analytical distribution to a relatively limited number of LHS sample points is to use a PCE approach to generate a surrogate model from an approximate polynomial series. The surrogate model, then, can be quickly run for a much higher number of samples and statistical evaluations can be performed directly on the surrogate data in a nonparametric fashion without any assumptions as to the distribution form. Here, around 100 – 200 CEX2D runs were simulated per case to generate a PCE-derived surrogate model again via the Dakota framework. This surrogate PCE model was then used to generate at least 10000 LHS points to exceed the number of cases necessary to calculate the nonparametric one-sided tolerance intervals for up to "3-sigma" (~99.7%) proportion of the population. Sample results of the PCE approach are plotted against the prior LHS results in Figure 9. Only minor differences between the two approaches are seen. Here, the PCE results estimate around 20 – 30 kg or 2 – 4% of higher throughput than the LHS predictions for TL40 shown above in Table 2.

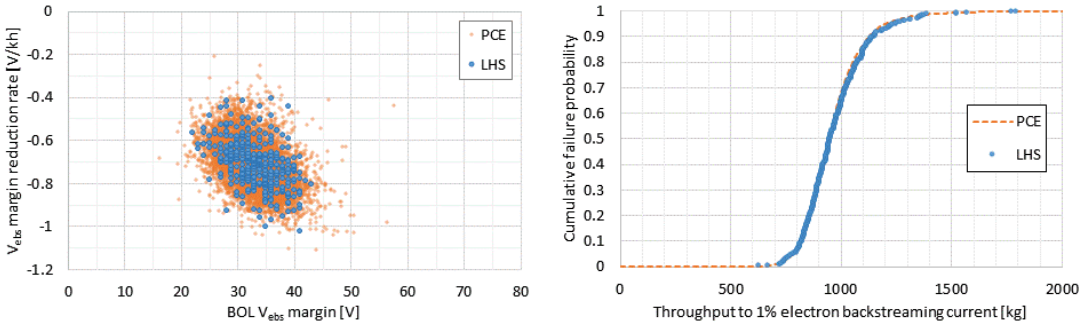


Figure 9: Comparison of PCE and LHS results for TL40

These UQ analyses also provide insight into which input parameters have the most impact on the factors determining service life from loss of electron backstreaming margin. Various sensitivity analyses can show the influence of each variable independently and in conjunction with the others. Perhaps the most straightforward approach is to generate simple scatter plots. Figure 10 and Figure 11 show how the barrel erosion rate varies for TL37 and how V_{ebs} margin varies for TL40, respectively, across each of the fourteen input parameters. Another more quantitative approach is to calculate the Sobol variance-based sensitivity indices which quantify how much the variance in the output is dependent on the variance of a given input by itself (main effect index) or on the variance of a given input including interactions with all of the other input variables (total effect index). Since proper calculation of these indices require many hundreds to thousands of data points, the Dakota PCE results are used and the total effect indices are presented in Figure 12. The main indices, which do not account for variable interaction effects, are similar indicating the contributions of the input uncertainties to the output uncertainty are relatively independent and higher-order interaction effects are minor. In general, these different approaches to sensitivity analyses show similar outcomes where the beamlet current density, mass flow rate, and accelerator grid aperture radius are the primary drivers for barrel erosion rate for TL37. For initial V_{ebs} margin for TL40, the beam and accelerator grid voltages along with most grid geometry parameters have noticeable influence. The relative lack of parameter overlap between the two sets of results also reflect and further support the basis of relative independence between at least these worst-case TLs as was shown earlier in Figure 7.

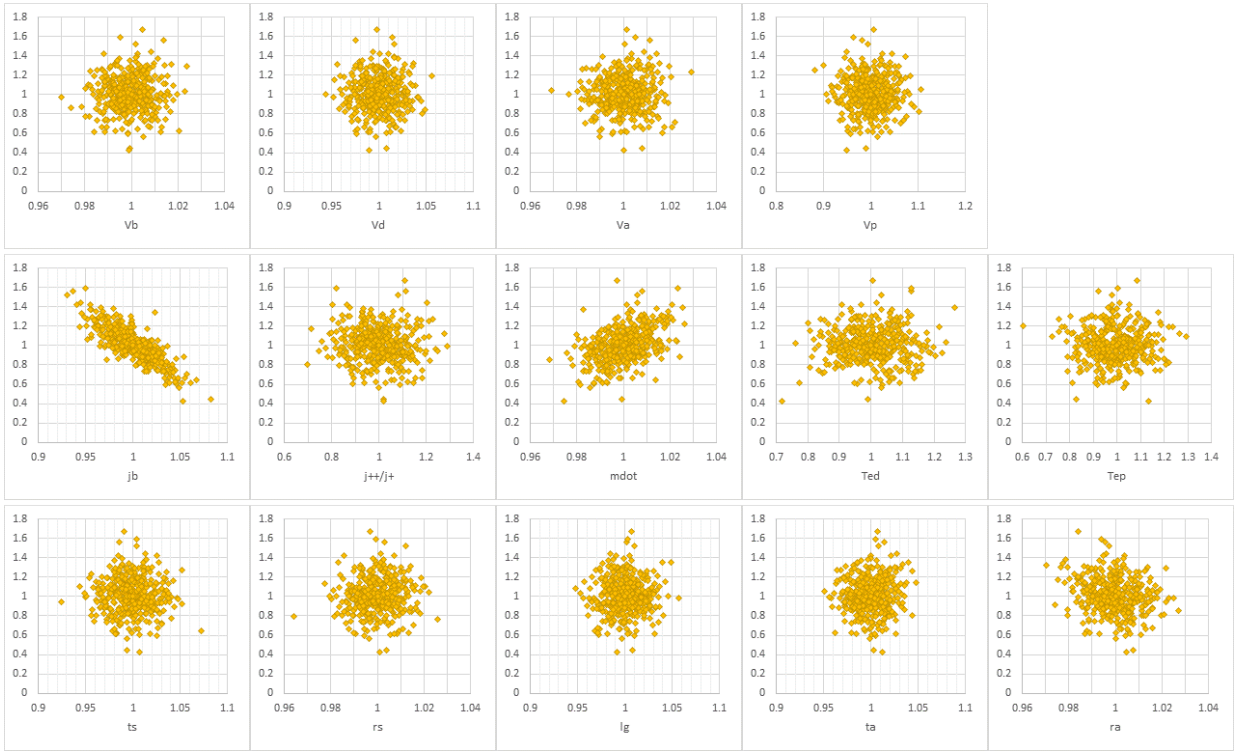


Figure 10: Normalized scatterplots of barrel erosion rate for TL37

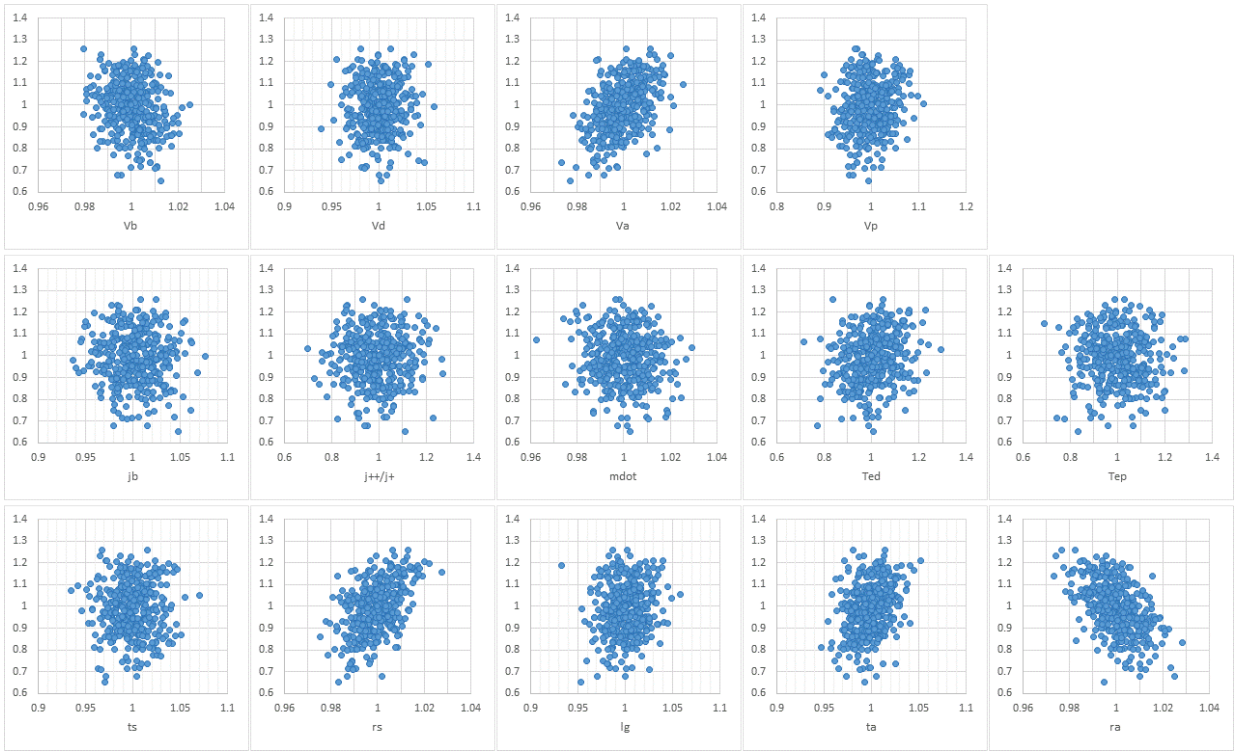


Figure 11: Normalized scatterplots of initial V_{ebs} margin for TL40

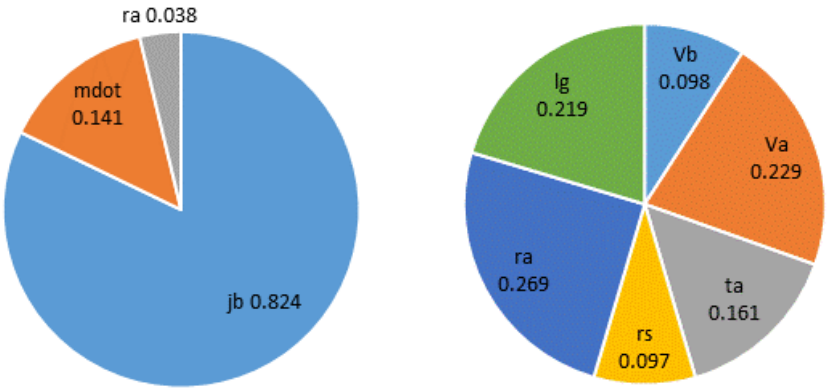


Figure 12: Sobol total indices of the primary contributors to barrel erosion rate for TL37 (left) and initial V_{ebs} margin for TL40 (right)

It should be clearly noted that these sensitivities—and indeed the whole set of results of these UQ analyses—are a strong function of the assumed input uncertainty variances. For example, other variables not shown in Figure 12 certainly still influence both barrel erosion rate and initial V_{ebs} margin, but based on the aleatory ranges estimated from their sources listed in Table 1, they do not have as an appreciable effect. If their variances were larger—for example, if the manufacturing tolerances were relaxed or an out-of-specification part was accepted—then certainly those other parameters could have an oversized effect on the end result than depicted above. Within the assumed aleatory variances, however, the variables highlighted above appear to have the strongest effect on the electron backstreaming outcomes. It should also be noted that the sensitivity results in Figure 10 through Figure 12 are specific for TL40 for initial V_{ebs} margin and TL37 for barrel erosion rate as they are the worst-case for each, respectively. These sensitivities change as a function of TL, where changes in relative perveance, beam-to-total grid voltage ratio, and other factors then subsequently affect which input variables will have more impact on barrel erosion and initial V_{ebs} margin. Depending on a specific mission throttle profile, the primary sensitivities can be re-evaluated to understand which parameters have the most influence for that particular situation.

As more thrusters and system components are manufactured, inspected, and tested, some of these parameters and their applied aleatory uncertainties will likely improve and be refined from the additional data. In particular, the realized manufacturing tolerances will be better understood from component-level inspections, the beam current density profile from thruster acceptance tests, and the voltage and mass flow from PPU and mass flow controller acceptance testing. Should service life be a strong driving factor for application of NEXT for a particular mission or application, then these tests and inspections offer a mitigation option to screen certain components and reject ones that unfavorably impact the expected service life. For example, extra grid sets can be manufactured for a given mission and the ones with the best qualities for long service life can be implemented on the flight thruster. Similar approaches can be applied at the discharge chamber assembly for more uniform beam current density profiles, PPU for more accurate voltages, and feed system for tighter controlled propellant flow rates.

IV. Summary and recommendations

The uncertainty quantification analysis approach provides an expanded understanding of the distribution of the expected service life of NEXT for the electron backstreaming failure mode. Instead of a single point estimate with an unknown level of conservatism and true margin, the generation of service life distributions provide a range of expected throughput capabilities based on the level of acceptable risk for a given mission. Estimates of the worst-case scenarios from an electron backstreaming standpoint are provided above in Figure 8 and Table 3. It should be noted that all other usage conditions will have substantially more life, and for future missions this analysis should be performed for a mission's specific operational throttle profiles to generate the tailored expected throughput capability and probabilities to achieve mission requirements.

The corresponding sensitivity analysis also provides insight into the significant parameters that more strongly influence the outcomes. These results can be used to update the requirements or provide screening criteria as a preemptive mitigation approach if service life is a driving factor. Of course, other mitigation options are available to preclude mission failure due to excessive electron backstreaming in flight. The first is to shift TLs when the V_{ebs} margin approaches zero. As noted above, electron backstreaming is a strong function of the throttle set point, and the

easiest and most straightforward mitigation is to change the TL to one with a higher inherent V_{ebs} margin (generally one with a lower beam current and/or voltage). Of course, the resulting consequence to the mission is the potential loss of an optimized Isp, thrust, or trajectory towards the end of thruster life, but if acceptable to the mission, this offers a relatively easy workaround.

An alternative mitigation when the V_{ebs} margin approaches zero is to adjust the accelerator grid voltage to increase the margin to electron backstreaming. The NEXT PPU is capable of accommodating accelerator grid voltages up to -525 V, which offers more than a 2x margin over the nominal setting for most of the throttle table except for the very low end of TL01 – 03 which already have hundreds of volts of V_{ebs} margin to begin with. Even a relatively modest change of 10 – 20 V can significantly extend life by a few hundred kilograms of additional throughput. The consequences of this mitigation approach include increased sputter erosion of the accelerator grid by an estimated 10 – 20% for pit-and-groove and roughly 5 – 10% for barrel erosion. There will also be minor impacts to thruster performance as a result of the accelerator grid voltage adjustment. While these resulting impacts should be closely examined for the mission at hand, adjusting the accelerator grid voltage is another relatively simple approach that could add hundreds of additional kilograms of propellant throughput before failure from electron backstreaming.

Apart from performing the analysis for specific mission use profiles and updating the aleatory uncertainties as more data are generated from additional thruster builds and tests, other avenues of future work to improve the analysis are certainly present. Continued scrutiny of the various epistemic uncertainties is recommended, particularly of the erosion rate based on assumed neutral number density distributions, sputter yield curves, and redeposition models. Further improvements to the core CEX2D model to enhance physical fidelity would also improve confidence. This includes additional examination of the thruster grids wear rates and assumed changes in boundary conditions over time. Probabilistic assessment of other life limiting mechanisms for NEXT, in particular failure from pit-and-groove erosion, is also planned to be completed.

Acknowledgments

This work was funded by the NEXT-C project, which is led by NASA GRC under NASA's Science Mission Directorate. The research described in this paper was carried out in part at the Jet Propulsion Laboratory, California Institute of Technology, under a contract with the National Aeronautics and Space Administration.

References

[1]Dankanich, J. W., Brophy, J. R., and Polk, J. E., "Lifetime qualification standard for electric thrusters," *45th AIAA/ASME/SAE/ASEE Joint Propulsion Conference and Exhibit*, AIAA-2009-5095, 2009.

[2]Yim, J. T., Soulas, G. C., Shastry, R., Choi, M., Mackey, J. A., and Sarver-Verhey, T. R., "Update of the NEXT ion thruster service life assessment with post-test correlation to the long-duration test," *35th International Electric Propulsion Conference*, IEPC-2017-061, 2017.

[3]Van Noord, J. L., and Herman, D. A., "Application of the NEXT ion thruster lifetime assessment to thruster throttling," *44th AIAA/ASME/SAE/ASEE Joint Propulsion Conference and Exhibit*, AIAA-2008-4526, 2008.

[4]Van Noord, J. L., "Lifetime assessment of the NEXT ion thruster," *43rd AIAA/ASME/SAE/ASEE Joint Propulsion Conference and Exhibit*, AIAA-2007-5247, 2007.

[5]Brophy, J. R., Polk, J. E., Randolph, T. M., and Dankanich, J. W., "Lifetime qualification of electric thrusters for deep-space missions," *44th AIAA/ASME/SAE/ASEE Joint Propulsion Conference and Exhibit*, AIAA-2008-5184, 2008.

[6]Goebel, D. M., Polk, J. E., Wirz, R. E., Snyder, J. S., Mikellides, I. G., Katz, I., and Anderson, J., "Qualification of commercial XIPS ion thrusters for NASA deep space missions," *44th AIAA/ASME/SAE/ASEE Joint Propulsion Conference and Exhibit*, AIAA-2008-4914, 2008.

[7]Brophy, J. R., "Propellant throughput capability of the Dawn ion thrusters," *30th International Electric Propulsion Conference*, IEPC-2007-279, 2007.

[8]Brophy, J. R., Katz, I., Polk, J. E., and Anderson, J. R., "Numerical simulations of ion thruster accelerator grid erosion," *38th AIAA/ASME/SAE/ASEE Joint Propulsion Conference and Exhibit*, AIAA-2002-4261, 2002.

[9]Wirz, R. E., Anderson, J. R., and Katz, I., "Time-dependent erosion of ion optics," *Journal of Propulsion and Power*, v. 27, n. 1, pp. 211-217, 2011.

[10]Wirz, R. E., Katz, I., Goebel, D. M., and Anderson, J. R., "Electron backstreaming determination for ion thrusters," *Journal of Propulsion and Power*, v. 27, n. 1, pp. 206-210, 2011.

[11]Polk, J., Chaplin, V., Yim, J., Soulas, G., Williams, G., and Shastry, R., "Modeling ion optics erosion in the NEXT ion thruster using the CEX2D and CEX3D codes," *36th International Electric Propulsion Conference*, IEPC-2019-907, 2019.

[12]Chaplin, V. H., Polk, J. E., Katz, I., Anderson, J. R., Williams Jr., G. J., Soulas, G. C., and Yim, J. T., "3D simulations of ion thruster accelerator grid erosion accounting for charge exchange ion space charge," *AIAA Propulsion and Energy Forum, 2018 Joint Propulsion Conference*, AIAA-2018-4812, 2018.

[13]Mikellides, I. G., Jongeward, G. A., Katz, I., and Manzella, D. H., "Plume modeling of stationary plasma thrusters and interactions with the Express-A spacecraft," *Journal of Spacecraft and Rockets*, v. 39, n. 6, pp. 894-903, 2002.

[14]Yim, J. T., "A survey of xenon ion sputter yield data and fits relevant to electric propulsion spacecraft integration," *35th International Electric Propulsion Conference*, IEPC-2017-060, 2017.

[15]Bolch, B. W., "More on unbiased estimation of the standard deviation," *The American Statistician*, v. 22, i. 3, p. 27, 1968.

[16]Herman, D. A., and Gallimore, A. D., "Discharge chamber plasma potential mapping of a 40-cm NEXT-type ion engine," *41st AIAA/ASME/SAE/ASEE Joint Propulsion Conference and Exhibit*, AIAA-2005-4251, 2005.

[17]Shastry, R., Herman, D. A., Soulas, G. C., and Patterson, M. J., "End-of-test performance and wear characterization of NASA's evolutionary xenon thruster (NEXT) long-duration test," *50th AIAA/ASME/SAE/ASEE Joint Propulsion Conference and Exhibit*, AIAA-2014-3617, 2014.

[18]Pollard, J. E., Diamant, K. D., Crofton, M. W., Patterson, M. J., and Soulas, G. C., "Spatially-resolved beam current and charge-state distributions for the NEXT ion engine," *42nd AIAA/ASME/SAE/ASEE Joint Propulsion Conference and Exhibit*, AIAA-2006-6779, 2006.

[19]Arthur, N. A., and Williams, G. J., "Near field probe measurements in the plume of a NEXT ion thruster," *36th International Electric Propulsion Conference*, IEPC-2019-167, 2019.

[20]Foster, J. E., Patterson, M. J., Pencil, E., McEwen, H., and Diaz, E., "Plasma characteristics measured in the plume of a NEXT multi-thruster array," *42nd AIAA/ASME/SAE/ASEE Joint Propulsion Conference and Exhibit*, AIAA-2006-5181, 2006.

[21]Soulas, G. C., and Patterson, M. J., "NEXT ion thruster performance dispersion analyses," *43rd AIAA/ASME/SAE/ASEE Joint Propulsion Conference and Exhibit*, AIAA-2007-5213, 2007.

[22]Thomas, R. E., Patterson, M. J., Crofton, M. W., and John, J. W., "NEXT ion propulsion system risk mitigation tests in support of the double asteroid redirection test mission," *AIAA Propulsion and Energy Forum, 2019 Joint Propulsion Conference*, AIAA-2019-4165, 2019.

[23]Sengupta, A., Brophy, J. R., Anderson, J. R., Garner, C., de Groh, K., Karniotis, T., and Banks, B., "An overview of the results from the 30,000 h life test of deep space 1 flight spare ion engine," *40th AIAA/ASME/SAE/ASEE Joint Propulsion Conference & Exhibit*, AIAA-2004-3608, 2004.

[24]Soulas, G. C., and Shastry, R., "Post-test inspection of NASA's evolutionary xenon thruster long duration test hardware: ion optics," *52nd AIAA/ASME/SAE/ASEE Joint Propulsion Conference and Exhibit*, AIAA-2016-4632, 2016.

[25]Polk, J. E., Anderson, J. R., Brophy, J. R., Rawlin, V. K., Patterson, M. J., Sovey, J., and Hamley, J., "An overview of the results from the 8200 hour wear test of the NSTAR ion thruster," *35th AIAA/ASME/SAE/ASEE Joint Propulsion Conference and Exhibit*, AIAA-1999-2446, 1999.

[26]Sengupta, A., Brophy, J. R., and Goodfellow, K. D., "Status of the extended life test of the Deep Space 1 flight spare ion engine after 30,352 hours of operation," *39th AIAA/ASME/SAE/ASEE Joint Propulsion Conference and Exhibit*, AIAA-2003-4558, 2003.

[27]Soulas, G. C., Kamhawi, H., Patterson, M. J., Britton, M. A., and Frandina, M. M., "NEXT ion engine 2000 hour wear test results," *40th AIAA/ASME/SAE/ASEE Joint Propulsion Conference and Exhibit*, AIAA-2004-3791, 2004.

[28]Adams, B. M., et al., "Dakota, a multilevel parallel object-oriented framework for design optimization, parameter estimation, uncertainty quantification, and sensitivity analysis," Sandia Technical Report SAND2014-4633, July 2014. Updated May 2018 (Version 6.8).

[29]*NIST/SEMATECH e-Handbook of Statistical Methods*, http://www.itl.nist.gov/div898/handbook/, 2013.